JOURNAL OF MATERIALS SCIENCE 30 (1995) 2352–2357

Mechanical and physical properties of post-creep, pitch-based carbon filaments

J. GERARD LAVIN
Dupont Co., Central Science & Engineering, Experimental Station, Wilmington, DE 19880-0302, USA

KEI KOGURE, G. SINES
Department of Materials Science and Engineering, University of California, Los Angeles, Los Angeles, CA 90024-1595, USA

New fabrication techniques have been developed for uniaxial creep specimens of pitch-based carbon filaments, with a matrix-free, test section. Pitch-based carbon filaments were found to plastically deform up to 73% elongation without necking. Mechanical properties and physical properties were changed significantly.

1. Introduction

DuPont carbon filaments E130, derived from pitch, have a much higher elastic modulus than PAN-based carbon filaments, and approach the strength of the strongest PAN-based carbon filaments. New fabrication techniques have been developed for uniaxial creep specimens of these pitch-based carbon filaments, which have matrix-free test sections. Under creep at high stress they exhibit large strain without necking.

2. Experimental procedure

2.1. Samples and techniques

The test section of the specimen was made from pitch-based, carbon fibre from DuPont, designated as E130 with 3000 filaments per bundle. The nominal filament diameter was 8.25 μm. E130 fibres have an ultra high elastic modulus of 896 GPa, which is close to the theoretical maximum value for graphite of 1020 GPa. The six yarn reinforced sections of the specimens, which form strong loops at the ends, were made from PAN-based carbon fibre bundles from Hercules. The fabrication techniques are described in [1].

The testing apparatus and procedures are the same as those used in the creep testing of PAN-based carbon filament [2]. The furnace is an electric resistance, carbon element furnace used at temperatures from 2200 to 2350 °C with a helium atmosphere. The single bundle test section was subjected to stresses from 300 to 800 MPa.

2.2. Creep responses

The creep responses of pitch-based carbon fibres are described in [1]. In the stress range 171–1103 MPa at a temperature of 2310 °C, the specimens demonstrated creep strain up to 73% without necking.

3. Results and discussion

3.1. Measurement of mechanical properties

3.1.1. Elastic modulus

The elastic modulus of carbon fibres is closely linked to the degree of preferred orientation of the crystallites; however, the strength of carbon fibres is thought to be controlled by defects, such as metallic impurities [3]. The modulus of carbon fibres is also determined by the degree of graphitization of the fibres. As the percentage of graphitization increases, the percentage of the microporosity, amorphous carbon and turbostratic phase decreases.

Ozbek *et al.* [4] reported that the elastic modulus of PAN-based carbon fibres from Courtaulds, which initially had a modulus of 180 GPa, increased up to 690 GPa after hot stretching for 2 h. The relationship between the elastic modulus and the reduction in cross-sectional area for PAN-based carbon fibre is shown in [4]. At the highest combination of load and temperature reported, namely a stress of 64 MPa and 3000 °C, the modulus increased from 180 to 690 GPa. An almost linear increase of modulus was obtained with induced strain, as measured by reduction in cross-sectional area for all loads and heating temperatures.

Francis *et al.* [5] found that an approximately linear relationship exists between preferred orientation and modulus for PAN-based carbon fibres from Courtaulds. That means there is a direct relationship between induced strain and preferred orientation, which results in an increase in the elastic modulus of the carbon fibres.

Table I shows the orientation angles and degree of graphitization that determine elastic modulus of carbon fibres [6]. The degree of graphitization was calculated from the interlayer spacing; it is assumed that shrinkage occurs between the (0 0 2) planes along the *c*-axis, while graphitization proceeds. Typical values of orientation angles for as-received E130 are 3.6–3.8°. The

0022–2461

TABLE I Filament characterization from X-ray diffraction measurement using conventional CuK_α Radiation

Specimen	Elongation (%)	Orientation angle (deg)	d_{002} (nm)	Degree of graphitization (%)	L_c (nm)
Control	–	3.1	0.3386	55.5	25.8
		2.9	0.3387		21.0
		4.1	0.3403		22.2
		2.6	0.3393		18.0
FPa	25	1.8	0.3388	60.4	45.1
FP1	25	1.7	0.3373	77.9	40.6
FP2	38	1.7	0.3373	77.9	44.4
FP3	47	2.3	0.3373	77.9	37.0
					36.2
FP4	73	1.6	0.3371	80.2	62.6

1.6–1.8° obtained on the authors' post-creep E130 are very low. A typical value of the degree of graphitization for as-received E130 is 55% [6]. The 80% obtained on post-creep E130 was much higher.

The above measurements indicate better orientation and higher graphitization after creep; therefore, the elastic modulus of the post-creep E130 should have increased. As Ozbek *et al.* pointed out on PAN-based carbon fibre, the elastic modulus depends on the induced strain on carbon fibres [4]. Johnson [7] also pointed to the relationship between the elastic modulus and the induced strain. For example, the authors' sample, FP4, underwent the highest plastic strain (73%), and had the best orientation angle (1.6°) and the highest degree of graphitization (80%). Johnson's work indicates that the author's specimen, FP4, probably had the highest elastic modulus.

The values of crystallite size, L_a, for as-received carbon fibres are related to physical properties and elastic modulus. Increase in magnitude of L_a during creep deformation causes positive magnetoresistance and reduction of electrical resistivity (see Sections 3.2.1. and 3.2.3.). Positive magnetoresistance of the post-creep E130 implies that L_a increased during the creep deformation (see Section 3.2.3.). Tanabe *et al.* [8] found a direct relationship between Young's modulus with the in-plane crystallite size L_a for pitch-based carbon fibres. The relation suggests that increase in magnitude in L_a of E130 carbon fibres after creep indicates higher elastic modulus of E130 carbon fibres. For PAN-based carbon fibres, the empirical relation has been used to relate elastic modulus to crystallite size, L_a [9]. The relation suggests that an increase in magnitude in L_a of PAN-based carbon fibres during creep deformation indicates an increase of the elastic modulus of PAN-based carbon fibres.

3.1.2. Tensile strength of post-creep carbon fibres compared with the strength of as-received fibres

S. Ozbek *et al.* [4] report that the strength of PAN-based carbon fibres from Courtaulds, that initially had a strength of 3.9 GPa (gauge length 25 mm), change after creep, depending on the creep temperature. They show the relationship between tensile strength and reduction in cross-sectional area for PAN-based carbon fibres. A trend of increasing strength with strain is evident from this figure, despite the scatter. A loss in strength from 3.9 GPa of the original fibres to 2 GPa is seen to occur when very little strain is induced; however, at larger strains the strength increases again. This indicates that the simultaneous application of heat treatment and deformation restores the fibre strength. At the highest combination of load and temperature reported, namely a stress of 64 MPa and 3000 °C, the tensile strength increases from 3.9 to 4.1 GPa.

Table II shows the authors' measurements of the tensile strength of the as-received, and the post-creep pitch-based carbon fibres, E130, along with their diameters. All tensile tests were carried out on an Instron testing machine. The diameter of these filaments was measured on a Vickers laser diffraction apparatus. Fifteen measurements were made of each monofilament and averaged. Fig. 1 shows the distributions of the diameters of the as-received and post-creep E130 carbon fibres. The as-received E130 carbon fibres had an approximate Gaussian distribution, with a mean diameter of 8.9 μm. The post-creep carbon fibres had a broad distribution, suggesting two populations. Eight filaments below 7.5 μm were found in the post-creep carbon fibres, versus two in the as-received carbon fibres. The change in carbon fibre diameter distribution is one of the evidences of super creep deformation.

Fig. 2 shows the relationship between the tensile strength and the filament diameter. The as-received E130 carbon fibres had an average strength of 3.5 GPa for a gauge length 25.4 mm, showing a trend of reduction of strength with increasing diameter. This trend also can be seen in as-received E130 carbon fibres with different gauge lengths as measured by Ma [10]. Ma also shows that, just like most brittle materials, the strength of E130 carbon fibres is strongly dependent on the testing gauge length. This indicates that the strength of carbon fibres is basically controlled by flaws. Weakest link theory, specifically the Weibull distribution, was used by Ma to process the testing data.

Post-creep E130 carbon fibres, even though tested at the shorter gauge length of 6 mm rather than the one of 25.4 mm used in the as-received tests, were lower in strength, average 2.4 GPa, than as-received, average 3.5 GPa. The decreased strength after creep might suggest generation of porosity or randomly

TABLE II Measurement of the tensile strength and diameters of post-creep and as-received E130 filaments (average of 15 measurements)

Sample	Post-creep specimen strain 25% Gauge length 6.35 mm		As-received Gauge length 25.4 mm	
	Diameter (μm)	Tensile strength (MPa)	Diameter (μm)	Tensile strength (MPa)
1	6.74	3799	7.98	2930
2	6.50	2627	7.93	3234
3	6.84	1586	9.14	3778
4	6.59	2786	8.66	3641
5	7.26	1862	7.90	3344
6	7.31	2303	8.51	3565
7	7.49	1931	9.46	3385
8			9.82	2751
9			10.00	4068
10			7.36	4344
11			7.36	3330
12			7.92	4054
Average	6.96 ± 0.39	2413 ± 745	8.51 ± 0.89	3537 ± 448

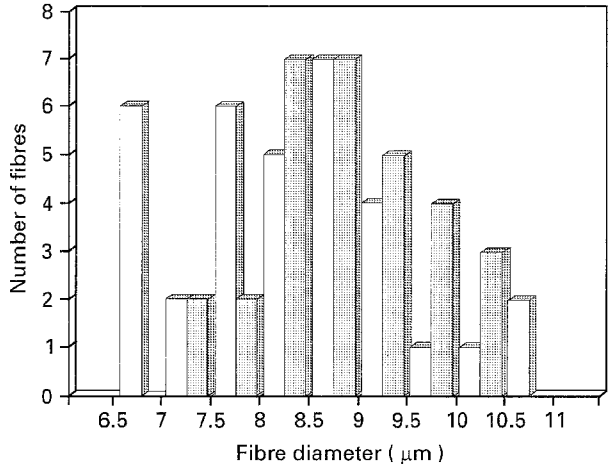

Figure 1 Distribution of diameters of the □ as-received and of the □ post-creep DuPont E130 carbon filaments.

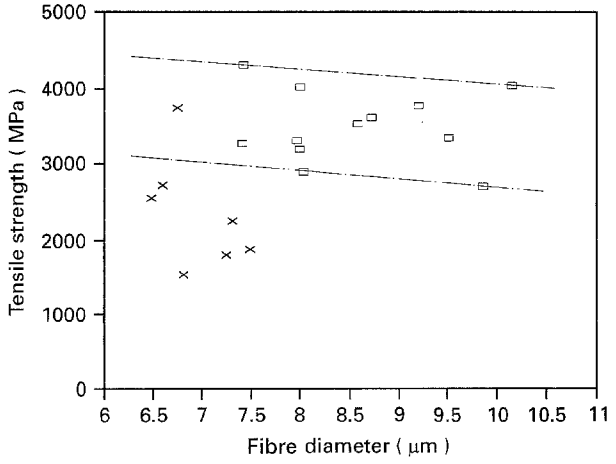

Figure 2 Tensile strength of (×) post-creep filaments, 6.35 mm gauge length, compared to the (□) as-received filaments 25.4 mm gauge length.

occurring defects during creep deformation. Decrease of strength during creep corresponds well with transmission electron microscopy (TEM) observations that show larger size of porosity [6]. However, as Ozbek *et al.* reported on PAN-based carbon fibres, the strength of pitch-based carbon fibre might be restored or might even increase at a combination of higher temperature and higher strain [4].

3.1.3. Dislocations in carbon fibres

The dislocations in carbon fibres are easy to observe in TEM. Especially by lattice fringes, single dislocations can be observed. These dislocations are observed in edge configurations. The ribbons can split, forming junctions of these ribbons so that a network of intersecting dislocations is set up. The graphitization process can be thought of as the gradual removal of stacking faults by annealing, and therefore removal of these basal dislocations [11].

Fig. 3, [6], shows dark field micrographs of post creep E130, which indicate the dislocations. Arrows indicate moiré patterns, which imply enlargement of single dislocations. Fig. 4 shows the enlargement of dislocations in moiré patterns. Dislocations might increase after creep. The sliding motion of crystallites during creep is compatible with edge dislocations. Dislocations do not necessarily promote this sliding motion of crystallites, nor do they inhibit the sliding motion. A dislocation mechanism for plastic deformation is necessary for the plastic deformation of strongly bonded structures. In the case of carbon fibres, however, interlayer movement between basal planes is easy due to weak van der Waals' bonding. In order for plastic deformation to occur in crystallites of carbon fibres, dislocations should move in the direction of maximum shear force, which is 45° inclined to the loading direction. Therefore, dislocations would have to exist perpendicular to the *c*-axis, and these have not been observed.

3.2. Measurement of physical properties

3.2.1. Electrical resistivity

The electrical resistivity of carbon fibres has been studied extensively as a diagnostic of the structural perfection of the fibres. The longitudinal resistivity

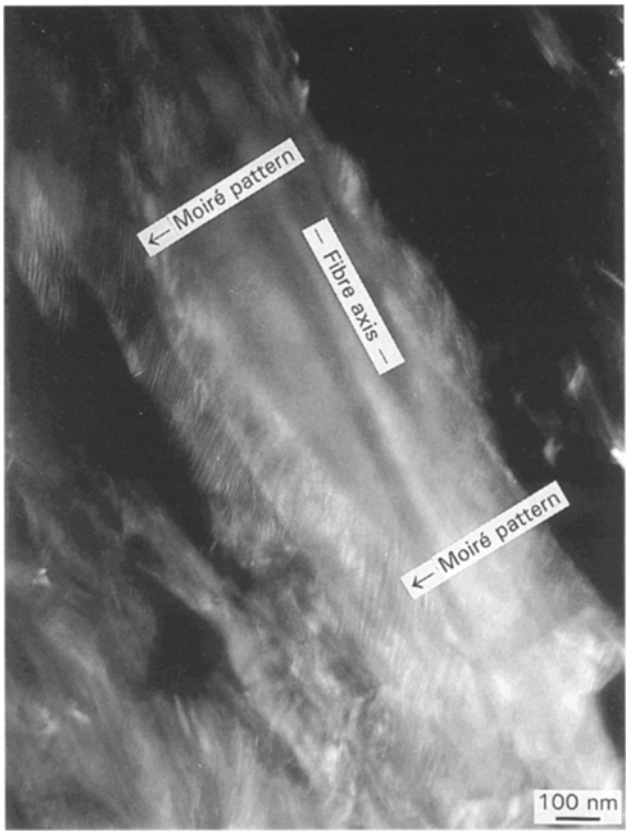

Figure 3 A (1 1 2) dark field electron micrograph of E130 carbon filament from an oblique section. Moiré patterns indicate dislocations. The arrow indicates the fibre axis.

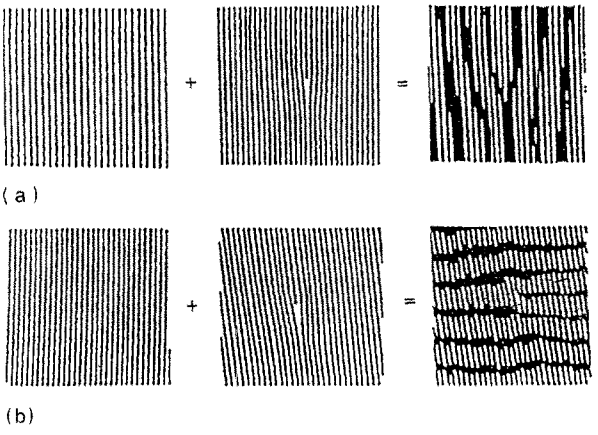

Figure 4 Enlargement of dislocations by moiré patterns.

was measured using a four point method, in which two current leads were attached to the ends of a single fibre, and two potential probes were introduced at about á quarter of the length of the fibre from each end. Contacts were applied with silver epoxy.

Electrical resistivity of as-received DuPont E130 was 400 $\mu\Omega$cm at 300 K. This value is comparatively low compared to that of other carbon fibres. Other pitch-based carbon fibres have values around 10000 $\mu\Omega$cm, while PAN-based carbon fibres have values of 6000 $\mu\Omega$cm. After creep deformation, the resistivity decreased to less than half of the original value, as indicated in Table III. This reduction of resistivity implies that crystallite size for the as-received, L_a, and post-creep, L_c samples increased during the creep test. As L_a increases, boundaries between the edges of the crystallites decrease. Therefore, hopping frequencies of electrons at the gap between crystallites decrease, and this reduces resistivity. As L_c increases, boundaries between the sides of the crystallites decrease, and again this reduces the frequency of hopping of the electrons. The relationship between L_a and electric resistivity has been investigated on PAN-based carbon fibre [12] and graphitizing carbon [13].

The degree of graphitization also relates to electrical resistivity. The increase of graphitization after creep from 55 to 80%, which means more orientated stacking of graphene planes with respect to rotation about the axis perpendicular to the planes, partially contributes to the reduction of electrical resistivity.

Grisdale *et al.* [14] investigated the relationship between electrical resistivity and crystallite orientation angles. They showed that crystallites with greater preferred orientation have lower electrical resistivity. After creep deformation, the orientation angles were reduced from 3.0 to 1.7° on carbon fibre E130, as indicated in Table I of [6]. This small difference of orientation angle would not contribute much to the more than 50% reduction of electrical resistivity that was observed. Therefore, reduction of electrical resistivity of carbon fibre E130 is predominantly due to increase of crystallite size.

3.2.2. Density and thermal conductivity of post-creep carbon fibres compared with those of as-received fibre

The carbon density can be related roughly to crystalline perfection, with the most highly ordered carbons approaching the mass density of single crystal graphite, which is 2.26 g cm^{-3}. The value of the density also can be related to degree of graphitization, elastic modulus and thermal conductivity of carbon fibres.

The as-received pitch-based carbon fibre, DuPont E130, which has an elastic modulus close to the theoretical value of single crystal graphite, has a high degree of graphitization. The density of DuPont E130 is 2.15 g cm^{-3}, which is approaching that of single crystal graphite. The density of commonly produced pitch-based carbon fibres is 2.02–2.06 g cm^{-3}, and the density of commonly produced PAN-based carbon fibres is 1.77–1.96 g cm^{-3} [11]. The high density of DuPont E130 is related to its high degree of graphitization.

Table IV gives the authors' measurements of the density of the as-received, and the post-creep, DuPont E130 carbon filaments. The density of these specimens was measured by the suspension of fibres in liquid of known density in a gradient tube at room temperature. The liquid of density 2.1 g cm^{-3} is obtained from the mixture of carbon tetrachloride (CCl_4) and bromoform ($CHBr_3$) in volume ratio of 270:180. The liquid density of 2.2 g cm^{-3} is obtained from the mixture of the same chemicals in volume ratio of 238:212. The degree of graphitization and calculated thermal conductivity of each specimen are also presented in Table IV. Thermal conductivity,

TABLE III Electrical resistivity and magnetoresistance of as-received and post-creep DuPont E130 carbon filaments

Specimen	Strain (%)	Electrical resistivity (μΩ cm)	Magnetoresistance (0.6 T, 20 °C)
FP1	25	343	0
FP2	38	330	0
FP3	47	185	0
FP4	73	191	+ 0.1%
As-received	–	392	0

TABLE IV Density and calculated thermal conductivity of as-received & post-creep, DuPont E130

Specimen	Strain (%)	Degree of graphitization	Density g/cm^3	Thermal conductivity (W/mK)
FP1	25	77.9	2.164	408
FP2	38	77.9	2.155	424
FP3	47	77.9	2.166	722
FP4	73	80.2	–	703
As-received	–	60.4	2.150	351

k (W/m^{-1}K^{-1}), of each specimen was calculated using the empirical equation

$$k = [440\,000/(\sigma + 258)] - 295 \quad (7)$$

where σ (μΩ cm) is the measured electrical resistivity. The equation has been shown to fit very well for DuPont and Amoco pitch-based carbon fibres [15].

The density of E130 is the same statistically whether it is as-received or post-creep, although the degree of graphitization increases from 56 to 80% after creep and the thermal conductivity increases from 381 to 685 W/m^{-1}K^{-1} after creep. [Of all materials, diamond and graphite (in-plane) exhibit the highest known room temperature thermal conductivity of 1950 W/m^{-1}K^{-1}; silver, the best metallic conductor, exhibits a thermal conductivity of only 420 W/m^{-1}K^{-1}.]

The fact that the same bulk density exists after creep as before creep suggests the generation of porosity during creep deformation. The density decrease from increase of porosity is compensated by the higher local density of the more highly graphitized carbon. Generation of porosity corresponds well with the decrease of strength after creep (see Section 3.1.2) and with the TEM observations in [6]. Comparing TEM micrographs of longitudinal sections of an as-received and a post-creep E130 carbon fibre, the one of the post-creep E130 carbon fibre has larger well developed graphitized regions and exhibits more porosity than the one as-received [6]. This corresponds well with the observation that there is no increase in density after creep.

3.2.3. Magnetoresistance

Magnetoresistance measurements provide a very sensitive way to determine the degree of order in carbon fibres. Fibres with high structural perfection show large positive magnetoresistance; smaller values correspond to more disordered graphite. Positive magnetoresistance is indicative of an increase in cyclotron frequency, which increases the resistivity by reducing the drift velocity between collisions. When three-dimensional order is low, the fibres assume a turbostratic structure where there is less interlayer site correlation between graphene planes. The magnetoresistance is negative for turbostratic carbon. DuPont pitch-based carbon fibres are considered to be less turbostratic, but they exhibit negative magnetoresistance. Data show, surprisingly, that the magnitude of the negative magnetoresistance increases as the disorder decreases from the E35 fibres to the E120 fibres at 4.2 and at 77 K [16]. For E130 fibres having more structural perfection than E120, the magnitude of the negative magnetoresistance decreases, especially at 77 K [16]. Magnetoresistance data give a measure of the proportion of turbostratic regions in the fibres and also the degree of disorder in their microstructure: boundaries, voids, amorphous regions, magnetic impurities, etc. [16].

The most commonly used model to explain the negative magnetoresistance of graphite has been the Bright model [17]. This model is based on the assumption that the electronic structure for turbostratic carbon should be nearly two-dimensional. As a consequence, the magnetic field induces changes in the electronic density of states, which lead to an increase in carrier concentration.

Bayot *et al.* [18] have proposed an alternative explanation for this peculiar behaviour. Their approach was based on the weak localization effects resulting from weak disorder in electronic systems. Their suggestion was that the two-dimensional, weak localization effects observed in those materials is due to the turbostratic phase, i.e. the quasi two-dimensional phase.

Magnetoresistance is more sensitive to differences in the microstructure of graphitized carbon than is X-ray diffraction. Negative magnetoresistance is sensitive to out-of-plane correlations, while resistivity is more sensitive to in-plane order [11].

By the four terminal method, passing a direct current under the magnetic field of 0–1 T applied perpendicular to the fibre axis, the transverse magnetoresistance of the fibres was obtained. As-received E130 filaments show negative magnetoresistance, due to the heterogeneous structure of the filaments as indicated in TEM micrograph [6]. The micrograph shows the disordered regions which contribute to negative magnetoresistance, and well developed regions which contribute to positive magnetoresistance. On average, the magnetoresistance of the filaments is negative at low temperature.

After creep deformation, however, magnetoresistance became positive (0.6 T, 300 K). During creep, the sliding motion of crystallites helps to join one layer at a time, i.e. epitaxial growth of c-axis alignment (ABABAB,...). Thus graphitization takes place progressively. As L_a of crystallites increases, L_c increases to put the layers in the right positions, by finding potential minima. Therefore, after creep, the carbon fibre E130 is mainly composed of graphitic structure. The results of X-ray diffraction and TEM observation, as previously described in [5], also reveal the increased graphitization.

4. Conclusions

The measured increases of preferred orientation, crystallite size and the increased graphitization resulting from the creep of the E130 caused increased electrical conductivity, which should cause an increase in the elastic modulus. The measured strength was reduced, perhaps by the increased porosity. An empirical equation indicates increase of thermal conductivity after creep.

Acknowledgements

The writers want to extend their special appreciation to DuPont Fibers, who supported the research by a gift and provided their E130 carbon fibres. Measurements of mechanical and physical properties of carbon fibres were made by them in their facilities.

References

1. K. KOGURE, PhD Dissertation, University College of Los Angeles (1992).
2. G. SINES, Z. YANG and B. VICKERS, *Carbon* **27** (1989) 403.
3. S. OHTANI, *J. Soc. Automotive Engng Jpn* **45** (1991) 46.
4. S. OZBEK, G. M. JENKINS and D. H. ISAAC, in "20th Biennial Conference on Carbon, Extended Abstracts", Santa Barbara (American Carbon Society, University Park, OH, 1991) p. 308.
5. J. G. FRANCIS, G. M. JENKINS and D. H. ISAAC, in "20th Biennial Conference on Carbon, Extended Abstracts", Santa Barbara (American Carbon Society, University Park, OH, 1991) p. 246.
6. K. KOGURE, J. G. LAVIN and G. SINES, in "21st Biennial Conference on Carbon, Extended Abstracts", Buffalo (American Carbon Society, University Park, PA, 1993) p. 18.
7. W. JOHNSON, in "Proceedings of the Third Conference of Industrial Carbon and Graphite" (Society of Chemical Industry, London, 1970) p. 447.
8. Y. TANABE, E. YASUDA, K. YAMAGUCHI, M. INAGAKI and Y. YAMADA, *TANSO* **147** (1991) 66.
9. M. GUIGON, A. OBERLIN and G. DESARMOT, *Fibre Sci. Technol.* **20** (1984) 177.
10. L. MA, MSc Thesis, University College of Los Angeles (1990).
11. M. S. DRESSELHAUS, C. DRESSELHAUS, K. SUGIHARA, L. L. SPAIN and H. A. GOLDBERG, "Graphite Fibers and Filaments", Springer Series in Materials Science (Springer, Berlin, 1988).
12. A. SHINDO, Report of the Government Industrial Research Institute, Osaka, No. 317, 1961.
13. J. C. BOWMAN, J. A. KRUMHANSL and J. T. MEERS, "Industrial Carbon and Graphite" (Society of Chemical Industry, 1958) p. 52.
14. R. O. GRISDALE, A. C. PFISTER and W. VAN ROOSEBROEK, *Bell Syst. Technol. J.* **30** (1951) 271.
15. J. G. LAVIN, D. R. BOYINGTON, J. LAHIJANI, B. NYSTEN and J.-P. ISSI, *Carbon* **31** (1993) 1001.
16. B. NYSTEN, J.-P. ISSI, R. BARTON, D. R. BOYINGTON and J. G. LAVIN, *J. Phys. D, Appl. Phys.* **24** (1991) 714.
17. A. A. BRIGHT, *Phys. Rev. B* **20** (1979) 5142.
18. V. BAYOT, L. PIRAUX, J.-P. MICHENAUD and J.-P. ISSI, *ibid.* **40** (1989) 3514.

Received 17 January
and accepted 8 September 1994